THE JOURNAL OF BIOLOGICAL CHEMISTRY VOL. 290, NO. 8, pp. 5127–5140, February 20, 2015
© 2015 by The American Society for Biochemistry and Molecular Biology, Inc. Published in the U.S.A.

Induced Expression of FcγRIIIa (CD16a) on CD4$^+$ T Cells Triggers Generation of IFN-γ^{high} Subset*[S]

Received for publication, July 29, 2014, and in revised form, December 29, 2014 Published, JBC Papers in Press, January 2, 2015, DOI 10.1074/jbc.M114.599266

Anil K Chauhan[‡§1], **Chen Chen**[‡], **Terry L. Moore**[‡], **and Richard J DiPaolo**[§]

From the [‡]*Division of Adult and Pediatric Rheumatology and* [§]*Department of Molecular Microbiology and Immunology, Saint Louis University School of Medicine, St. Louis, Missouri 63104*

Background: Fcγ-receptors play an important role in the immune responses.
Results: We show that upon activation by immune complexes peripheral CD4$^+$ T-lymphocytes express FcγRIIIa and produce a subset that express high levels of IFN-γ.
Conclusion: We describe for the first time a role for FcγRIIIa in CD4$^+$ T-cell differentiation.
Significance: This CD4$^+$FcγRIIIa$^+$IFN-γ^{high} subset will be critical in understanding the underlying autoimmune pathologies.

Whether or not CD4$^+$ T-cells express low affinity receptor FcγRIIIa (CD16a) in disease pathology has not been examined in great detail. In this study, we show that a subset of activated CD4$^+$ T-cells in humans express FcγRIIIa. The ligation of FcγRIIIa by immune complexes (ICs) in human CD4$^+$ T-cells produced co-stimulatory signal like CD28 that triggered IFN-γ production. The induced expression of FcγRIIIa on CD4$^+$ helper T-cells is an important finding since these receptors via ITAM contribute to intracellular signaling. The induced expression of FcγRIIIa on CD4$^+$ T helper cells and their ability to co-stimulate T-cell activation are important and novel findings that may reveal new pathways to regulate adaptive immune responses during inflammation and in autoimmunity.

Fc receptors (FcRs)[2] play a central role in the pathogenesis of autoimmunity (1–3). FcRs are critical for both afferent and efferent phases of the immune response. These receptor proteins are widely expressed as pairs of activating and inhibitory receptors on monocytes, macrophages, neutrophils, eosinophils, natural killer (NK)-cells, dendritic cells, B cells, and mast cells (4). By engaging ICs, they trigger cell specific function via immunoreceptor tyrosine-based activation motif (ITAM) and/or inhibitory motif (ITIM) (1, 5). FcRs determine the functional outcome of immune cells by maintaining a balance of both activation and inhibitory signals (6). FcRs play a critical role in the phagocytosis, B cell activation, and cytokine release (7, 8). Polymorphic forms of FcRs that show low affinity for IC binding predispose for the development of systemic lupus erythematosus (SLE). Elevated levels of ICs are present in multiple disease conditions and contribute to the disease pathology by engaging FcγRIIIa on multiple cell types. These receptors are also targets for therapeutic interventions (9, 10). For example, FcRs are implicated in the anti-inflammatory response observed with intravenous immunoglobulin (IVIG) therapy (11, 12).

FcγRIIIa expression was observed in a small number of peripheral T-cells in healthy individuals in earlier studies (13, 14). Another study showed that IgM binding T-cells provided helper function, while IgG binding cells provided suppressor function (15). Two previous studies also emphasized an immunoregulatory role for FcR bearing T-cells during B cell-mediated immune responses (16, 17). FcR common γ-chain (FcR-γ) is the ITAM bearing signaling unit of FcεRI, FcγRI, and FcγRIIIa (7). This protein independently supported the complete development of peripheral T-cells in mice lacking the ζ-chain of the T-cell receptor (TCR) (18–20). In T-cells, FcR-γ chain form heterodimer with ζ-chain in the TCR complex. FcγRIIIa can signal using ζ-ζ chain, γ-γ chain homodimers, or ζ-γ chain heterodimer. These studies suggest a role for FcR-γ chain in T-cell physiology. Contrary to these reports, several reviews, including some recent, have emphasized the absence of FcRs on CD4$^+$ T lymphocytes (4, 9, 10).

Establishing the presence and the conditions under which FcγRIIIa appears in CD4$^+$ T-cells is important for understanding the role these receptors can play in T-cell-mediated pathological events. In these studies, we used multiple approaches to establish the presence of FcγRIII receptors on activated human CD4$^+$ T-cells. We characterized the presence of both FcγRIIIa and FcγRIIIb on activated CD4$^+$ T-cells. The presence of FcγRIIIa was observed both at the RNA transcript level and as a protein expressed on the cell membrane. IFN-γ is one of the most important endogenous mediators of immunity and inflammation. IFN-γ is also critical in limiting the inflammation associated tissue damage and modulate T helper cell differentiation. We demonstrate a role for FcγRIIIa in the production of IFN-γ by CD4$^+$ T-cells. We further demonstrate the enhanced binding of labeled ICs in two mice disease models.

EXPERIMENTAL PROCEDURES

Subjects—Heparinized blood was collected from normal subjects and systemic lupus erythematosus (SLE) patients with informed consent at the Saint Louis University Division of

* The study was funded by National Institutes of Health R01 Grant A1098114 (to A. K. C.).
[S] This article contains supplemental Fig. S1.
[1] To whom correspondence should be addressed: Division of Adult and Pediatric Rheumatology, Saint Louis University School of Medicine, Saint Louis, MO 63104. E-mail: chauhana@slu.edu.
[2] The abbreviations used are: FcR, Fc receptor; ITAM, immunoreceptor tyrosine-based activation motif; ITIM, inhibitory motif; TCR, T-cell receptor; SLE, systemic lupus erythematosus; AHG, aggregated human γ-globulin; IC, immune complex.

Rheumatology outpatient clinic. The SLE patients fulfilled 1982 revised criteria for diagnosis (21).

Cell Lines—Cell lines: Jurkat, an acute T-cell leukemia (TIB-152); P116, an acute T cell leukemia a ZAP-70 mutant (CRL-2676); Daudi, Burkit's lymphoma (CCL-213), and THP-1 acute monocytic leukemia (TIB-202) were obtained from ATCC.

Mice—The C57BL/6 mice were obtained from Jackson labs and maintained in disease free conditions at the animal facility of Saint Louis University. K/BxN mice (a mouse model for inflammatory arthritis) and TxA23 mice (an autoimmune gastritis model) were also housed in the same facility (22, 23).

Abs and Reagents—Antibodies against FcγRI/CD64 (antigen affinity-purified polyclonal, AF1257), FcγRIIIb/CD16b (antigen affinity-purified polyclonal, AF1597) and monoclonal anti-FcγRIIIa/b (CD16a/b) (MAB2546, clone 245536) were from R&D systems. A second anti-FcγRIII-PE (Clone 3G8) antibody that recognizes FcγRIII (CD16) was from eBioscience. Both of these monoclonal antibodies do not differentiate between FcγRIIIa and FcγRIIIb. The anti-CD4-PerCP Cy5.5 (clone RPA-T4), anti-IFN-γ-APC (clone 4S.B3), anti-T-bet-PE (clone eBio4B10), anti-CD3 (clone OKT-3), and anti-CD28 (clone CD28.2) were also procured from eBIoscience. Other common reagents, *N*-glycanase, custom primers, and cell culture reagents were obtained from IDT, Invitrogen, and Sigma chemicals. The reagents to purify the CD4$^+$ human naïve T-cells were procured from Miltenyi Biotec (Germany).

Preparation of CD4$^+$ T-cells and Monocytes—Human PBMC were isolated from 20 ml of heparinized blood using histopaque post 4 h of blood collection (Sigma Chemicals). RBCs were removed using lysis buffer (eBiosciences) and monocytes using a gradient of Nyco-prep (Aldrich). Cells were then plated overnight in Nunc culture dish with 10-cm diameter. The next day these cells were washed with phosphate-buffered saline (PBS)/EDTA and naïve CD4$^+$ T-cells were isolated using kit from Miltenyi Biotec (Germany). These cells were 93 to 96% pure based on CD4$^+$CD45RA$^+$ flow staining. The plate bound cells were washed three times with PBS and used to prepare lysates. More than 85% of these cells were CD14$^+$. Mouse cells were obtained from spleens or lymph nodes. Mouse CD4$^+$ T-cells were flow sorted.

Cell Propagation and Expansion—Purified 1 × 10^6/ml, CD4$^+$CD45RA$^+$ cells were maintained for 72 h in IL-2 (20 units) and thereafter activated in 96-well Nunc plates coated O/N at 4 °C with anti-CD3 (clone OKT3) at 0.5 μg/ml and anti-CD28 (clone CD28.2) at 1 μg/ml. Alternately, cells were treated with anti-CD3 (0.5 μg/ml) and ICs purified from pooled plasma (10 μg/ml) and C5b-9 (2.5 μg/ml) (24). All activations were carried out for 2 h in plain medium and terminated with complete medium. Cells were then cultured in complete RPMI medium with 10% FBS supplemented with 20 IU of IL-2 for 8 days before IC binding analysis. For mouse studies, cells were obtained from spleen and lymph nodes and analyzed the same day.

Preparation of Aggregated Human γ-Globulin, ICs, and Labels—Aggregated human γ-globulin (AHG) was prepared as previously described (25). Purified γ-globulin at 10 mg/ml in PBS was aggregated by heating at 63 °C for 30 min. The solution was centrifuged at 10,000 × *g* for 30 min, and the collected supernatant was re-centrifuged at 105,000 × *g* for 90 min. Thereafter, pellet was re-solubilized in PBS and centrifuged again at 10,000 × *g*. The supernatant fraction was collected, aliquoted, and frozen at −70 °C. The ICs were purified from patient plasma using an affinity matrix as described previously (26, 27). These purified ICs were previously compared with AHG and *in vitro* formed ova-anti-ovalbumin ICs in T cell activation assays (24). The protein content was measured using a micro BCA kit (Pierce Chemicals). The purified ICs or AHG were labeled with Alexa Fluor® 488 carboxylic acid, 2,3,5,6-tetrafluorophenyl ester as per the manufacturer's recommendation (Molecular Probes). The 14.04 μM dye/mg protein conjugates were obtained and used for flow and cell staining.

AHG and IC Binding Analysis of Peripheral of CD4$^+$ T-cells—For binding analysis, cells from individual human subject or cells pooled from three animals at a density of 1 × 10^6 cells were used. For flow analysis, cells were stained with Alexa Fluor labeled protein using 2 μg of total protein for staining 10^6 cells at room temperature for 30 min. After staining, cells were fixed using fixation buffer (eBioscience) for 30 min, and data were acquired in LSRII flow cytometer (BD Biosciences). We used 0.5 to 5 μg of AHG-Alexa Fluor 488 for titration of AHG binding. For competitive inhibition of AHG binding, the cells were pretreated with various amounts of anti-FcγRIIIa/b monoclonal antibody (R& D Systems, clone 245536, Product MAB2546) ranging from 0.5 to 20 μg for 1 h at room temperature and thereafter labeled using 2.5 μg of labeled AHG, 30 min at room temperature. Isotype mouse Ig2a was used as control for inhibition studies. Same conditions were used for inhibition with anti-FcγRI, an affinity purified polyclonal (R&D Systems, Product AF1257); anti-FcγRIIIb, an affinity-purified polyclonal (R&D Systems, Product AF1597) and goat F(ab)$_2$ as control. For surface staining of FcγRIII, we also used anti-CD16-PE conjugate (clone 3G8) as per manufacturer recommendation (Invitrogen, Product MHCD1604). For other surface markers the antibody conjugates with appropriate dyes were used per the manufacturer's recommendation. Data analysis was carried out using FlowJo software.

Cell Staining using FcγRIIIa/b and FcγRIIIb Antibodies—A total of 0.5 × 10^6 cells were washed with cold PBS, afterward fixed in 3% formaldehyde for 15 min at room temperature. Fixed cells were then permeabilized using 95% methanol for 30 min on ice and 10 min at −20 °C. After washing, blocking was performed with 1% BSA and 2.5% species-specific serum diluted in PBS at room temperature for 1 h. These cells were then incubated with primary antibody at a dilution of 1:100 for 1 h at room temperature. For co-staining, a monoclonal antibody recognizing the FcγRIIIa/b (Clone 245536) and a polyclonal FcγRIIIb (R&D Systems, Product AF1597) were used. Subsequently cells were incubated with anti-mouse Alexa® Fluor 405 and anti-goat Alexa® Fluor 594 secondary antibodies at a dilution of 1:200 at room temperature for 1 h. Co-localization was carried out using Olympus FV-1000 software. Cells were examined at 400 and 630× magnification in fluorescent (Leica, DM400B) or confocal microscope (Olympus, FV-1000). Percentages of positive cells were calculated in two fields in three independent experiments.

Immunoblotting—Four million non-activated or activated CD4$^+$ T-cells and THP-1 cells were washed with PBS and lysed

in 0.5 ml of RIPA buffer (Tris-HCl: 50 mM, pH7.5; Nonidet P-40: 1%; Na-deoxycholate: 0.25%; NaCl: 150 mM; EDTA: 1 mM; PMSF: 1 mM, and protease inhibitors pepstatatin, leupeptin, aprotinin: 1 μg/ml each). Thereafter, proteins were precipitated with 0.1 μg of monoclonal antibodies overnight at 4 °C. The antibody-bound proteins were captured with 50 μl of Protein G beads. Beads were washed three times with RIPA buffer and SDS-PAGE loading buffer was added to the beads. Proteins were electrophoresed on 4–12% SDS-PAGE and Western blotting was performed using polyclonal anti-FcγRIII antibody (Product sc-19357, Santa Cruz Biotechnology and AF1257 R&D Systems). After reduction with 50 mM DTT, alkylation was carried out with 125 mM iodoactamide for 1 h at room temperature. For *N*-glycanase digestion, beads with IPs obtained using clone 3G8, anti-FcγRIII antibody were suspended in 25 μl of 0.2 M Tris-HCl buffer, pH 8.0, containing 05% SDS, 50 mM 2-mercaptoethanol and heated for 3 min at 100 °C. Thereafter, 25 μl of 0.2 M Tris-HCl buffer containing 2 mM EDTA and 0.03% PMSF was added. The mixture then received 5 μl of 7.5% Nonidet P-40. The mixture was incubated overnight at 37 °C with 1 unit of *N*-glycanase (Sigma) and analyzed in Western blotting. For analysis of FcγRIII in protein lysates, 5 μg of protein in non-denaturing condition was electrophoresed and analyzed in Western blotting experiment.

RT-PCR for FCGR3 and DNA Sequencing—Total RNA was isolated from the cells using the total RNA isolation kit (Agilent Technologies). The cDNA was synthesized with high capacity cDNA synthesis kit (Applied Biosystems). Primers were designed based on the gene ID NM_001127596.1 (*FCGR3A*). The forward TCAAATGTTTGTCTTCACAG and reverse ATTCACCTGAGGTGTCACAG primer covering 504 to 831 nucleotide of *FCGR3A*, a 330-nucleotide length product covering exons 4 and 5 were used in the first PCR. The PCR product was purified from the agarose gel slice using Purelink gel extraction kit (Invitrogen). The 330-nucleotide PCR product was used as a template to re-amplify this product with M13-*FCGR3* hybrid primers forward primer TGTAAAACGACGGCCAGTCAAATGTTTGTCTTCACAG and reverse primer AGGAAACAGCTATGACCATATTCACGTGAGGTGTCACAG. The PCR product obtained was used to sequence both strands using M13 forward primer TGTAAAACGACGGCCAGT and reverse AGGAAACAGCTATGACCAT in automated sequencers using big dye. The sequence was aligned using BLAST at NCBI site.

qRT-PCR—For qRT-PCR studies, the gene expression assays were procured from IDT for *FCGR3A* (Hs.PT.49a.15478614.g), *Tbx21* (Hs.PT.58.20216516), and *ifng* (Hs.PT.58.3781960). GAPDH (Hs.PT.39a.22214836) was used as an endogenous control. The *FCGR3A* gene is designed based on *FCGR3A* gene variant and was purchased from Integrated DNA technologies (IDT). All other assays were also obtained from IDT. The qRT-PCR was performed using StepOne PCR machine with Fast RT-PCR mix (Applied Biosystems). Cells were maintained in complete medium with IL-2 (20 IU) for 3 days before activation. Activated cells were harvested at various time points for transcript analysis.

Cell Stimulation and IFN-γ Staining—For IFN-γ production, post activation as described earlier, cells were maintained in the presence of IL-2 (20 IU), and IL-12 (50 ng) (Peprotech) for each ml of complete medium. On day 8, cells were harvested and stained for CD4, IFN-γ, and T-bet. For intracellular cytokine staining, cells were stimulated with 1 μg/ml PMA and 2.5 μg/ml ionomycin for 4 h. Brefeldin 5 μg/ml (GolgiPlus BD) was added after 1 h of PMA/ionomycin stimulation. Cells were collected for staining post 3 h of addition of Brefeldin. After cell surface staining with anti-CD4, the intracellular staining for IFN-γ and T-bet was performed after fixation and permeabilization (fixation/permeabilization buffer, eBioscience), according to the manufacturer's suggested protocol.

RESULTS

Activated Peripheral Naïve CD4$^+$ T-cells Bind to Labeled AHG and ICs—ICs are natural ligand for low affinity FcRs. To confirm the presence of FcγRIIIa on CD4$^+$ T-cells, we first analyzed the binding of Alexa-Fluor®-488 labeled aggregated human γ-globulin (AHG), a model IC, and labeled ICs purified from SLE plasma, to the activated peripheral naïve CD4$^+$ T-cells. A donor analyzed in flow analysis for the binding of labeled ICs showed a 3-fold increase in IC binding to CD4$^+$ T-cells, that were treated with anti-CD3+anti-CD28 (17.5%), or anti-CD3+ICs+C5b-9 (18.2%). The anti-CD3-treated cells used as control showed 5.3% IC binding population (Fig. 1*A*). THP-1 cells that express FcγRIII also bound to labeled ICs (Fig. 1*B*, *red*). We further analyzed additional donors for both AHG and IC binding on day 8 post-activation. Both anti-CD3+anti-CD28 as well as anti-CD3+ICs+C5b-9 treatments showed statistically significant increase of AHG binding to the cells, at a p value of 0.046 and 0.03 ($n = 8$) and also for IC binding at a p value of 0.001 and0.0008 ($n = 9$), compared with anti-CD3-treated cells (Fig. 1, *C* and *D*). These results suggest that the activated CD4$^+$ T-cells expressed receptors that bound to AHG and ICs.

To further characterize the proteins to which the ICs and AHG bound, we stained activated CD4$^+$ T-cells with anti-FcRs specific antibodies. Since there is no specific antibody available that recognizes only FcγRIIIa, we utilized a monoclonal antibody (clone 245536, R&D Systems) that recognizes both FcγRIIIa and FcγRIIIb receptors and co-stained these cells with a second affinity-purified polyclonal antibody that recognize the FcγRIIIb (R&D Systems). Since, monoclonal antibody will occupy a single epitope on receptor, it will allow the binding of a polyclonal antibody to the alternate epitopes on receptor. A confocal image of a cell that was triple stained using ICs and antibodies against both receptors showed co-localized staining for ICs with both receptors on the cell membrane (Fig. 1, *E*, *F*, and supplemental Fig. S1). Further examination of activated cells from two fields in three independent experiments demonstrated staining of both FcγRIIIa and FcγRIIIb. A total of 36.67 ± 3.18% cells showed staining for FcγRIIIa, while 16.33 ± 3.78% cells stained for FcγRIIIb (Fig. 1*G*). Isotype control ($IgG_2\kappa$) and goat F(ab′)2 fragment did not demonstrate staining. Cells expressing FcγRIIIa always showed staining for FcγRIIIb (Fig. 1*G*).

We also examined the binding of a commonly used anti-FcγRIII antibody (clone 3G8), directly to CD4$^+$ T-cells in the PBMCs of fourteen SLE patients and *in vitro* activated purified peripheral naïve CD4$^+$ T-cells in three donors. In fourteen SLE

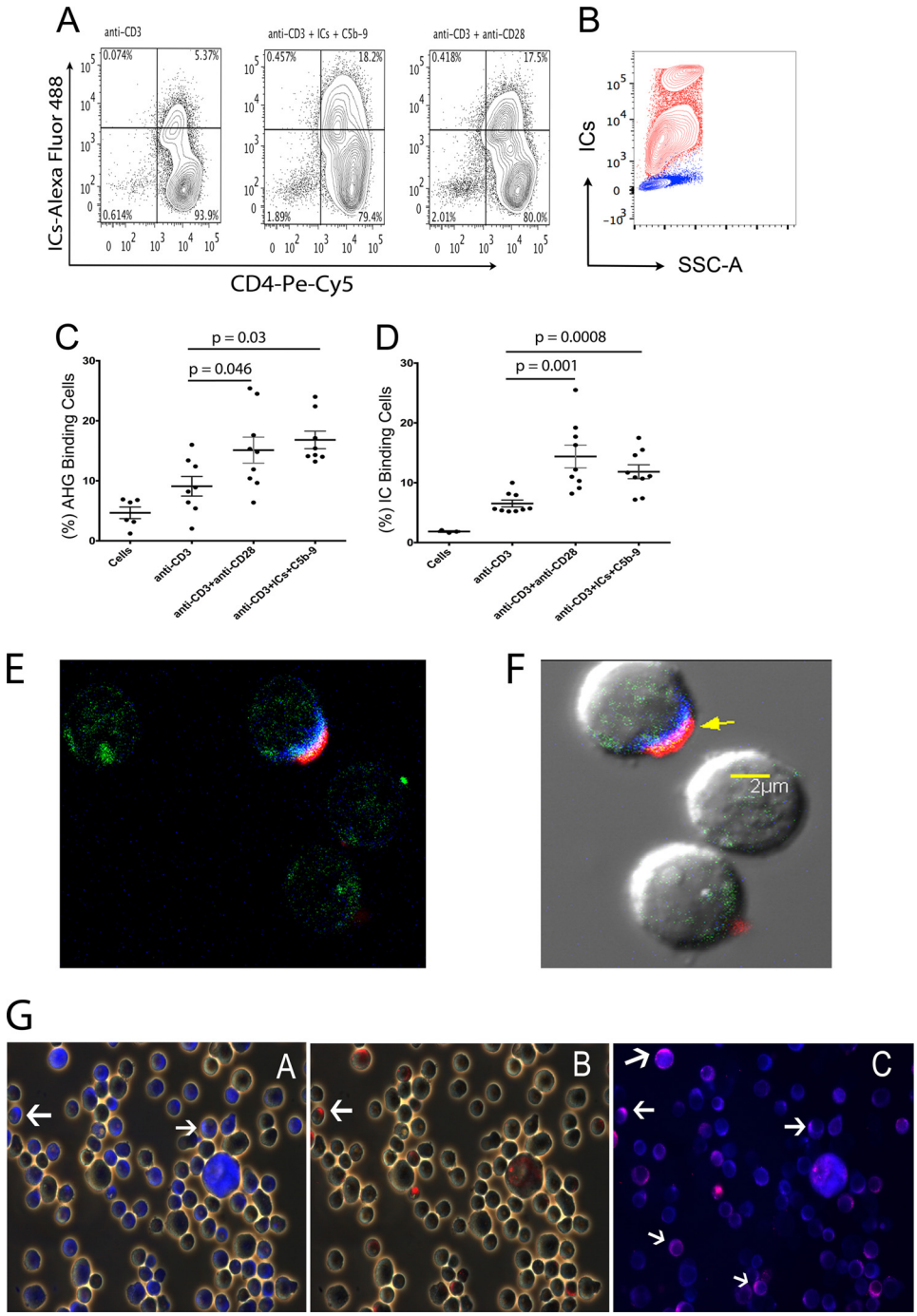

FIGURE 1. **Activated CD4$^+$ T-cells bind to AHG and ICs.** Flow cytometry analysis for Alexa-488-labeled AHG and ICs binding to activated naïve CD4$^+$ T-cells. *A*, cells activated in a donor with anti-CD3+anti-CD28 (17.5%) or anti-CD3+ICs+C5b-9 (18.2%) showed enhanced binding for ICs compared with cells treated with anti-CD3 (5.37%). *B*, THP-1 cells bound labeled ICs (*red*), unstained control (*blue*). *C*, binding of AHG to cells treated with anti-CD3+anti-CD28 showed statistically significant increase at a *p* value of 0.046, and treated with anti-CD3+ICs+C5b-9 at a *p* value of 0.03 compared with anti-CD3-treated cells, $n = 8$. *D*, binding of labeled IC to anti-CD3+anti-CD28 treated cells showed a statistically significant increase at a *p* value of 0.001 and in anti-CD3+ICs+C5b-9-treated cells at a *p* value of 0.0008 *versus* anti-CD3 treatment ($n = 9$). *E* and *F*, confocal image of a cell without and with DIC background, stained for IC-Alexa Fluor® 488 (*green*), anti-FcγRIIIa/b monoclonal-Alexa Fluor® 405 (*blue*), and anti-FcγRIIIb polyclonal-Alexa Fluor® 594 (*red*), (630× magnification). *G*, activated CD4$^+$ T-cells stained using anti-FcγRIIIa/b monoclonal-Alexa Fluor 405 (*blue*) and co-stained with anti-FcγRIIIb polyclonal-Alexa Fluor® 594 (*red*). *White arrows* point to blue and red stain. Cells demonstrated staining for both receptors (magnification 400×).

subjects examined by flow staining of PBMC using anti-CD16-PE (clone 3G8) demonstrated the presence of FcγRIII ranging from 0.21 to 10.8% with a mean ± S.E. of 3.33 ± 0.748 of CD4$^+$ T-cells (Fig. 2, *A–D*). *In vitro* activated cells using same antibody in anti-CD3+ICs+C5b-9 (17.4%) treated population also demonstrated 3-fold increase in anti-CD16 binding cells compared with cells that were treated with anti-CD3 (6.62%) alone (Fig. 2, *E* and *G*). Cells treated with anti-CD3+anti-CD28 showed small increase (Fig. 2*F*). THP-1 cells stained positive with anti-CD16 (Fig. 2*H*, *red*). These results are in concordance with IC binding population observed and further confirm the presence of these receptors in a subset of activated CD4$^+$

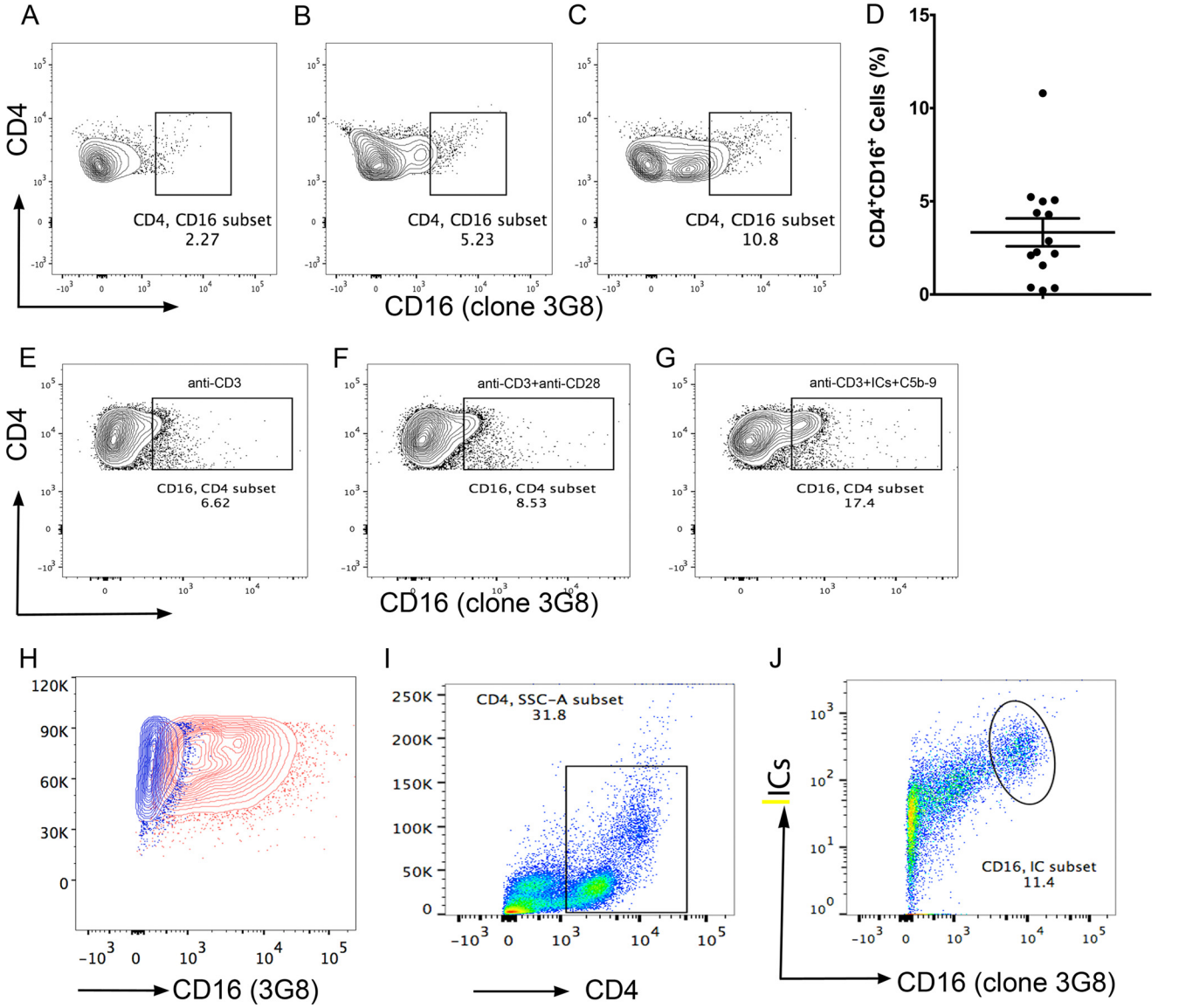

FIGURE 2. **A subset of CD4⁺ cells in PBMC binds to anti-CD16 (clone 3G8).** Flow analysis showed varied amount of cells bound to anti-CD16. CD16 expression shown in three donors (*A*) (2.27%); (*B*) (5.23%), and (*C*) (10.8%). A total of 14 subjects were analyzed in four separate experiments (*D*), combined analysis show 3.33 ± 0.748% (mean ± S.E.) cells bound to anti-CD16. Purified CD4⁺CD45RA⁺ T-cells stained with anti-CD16-PE on day 8 postactivation. Anti-CD3+ICs+C5b-9-treated cells showed ~3-fold increase in anti-CD16 binding (*G*) compared with anti-CD3 (*E*). A small increase in anti-CD3+anti-CD28 was also observed. THP-1 cells stained with anti-CD16 (*red*) and unstained control (*blue*) (*H*) CD4⁺ gated PBMC (*I*) CD4⁺ T-cells from PBMC show double staining for ICs-Alexa Fluor 488 and anti-CD16-PE (*J*) (shown 1/3 analyzed).

T-cells. Direct staining with monoclonal anti-FcγRIII antibody (3G8) and labeled ICs of CD4⁺ gated cells within the PBMCs from SLE patients showed double positive staining for antibody and ICs binding (Fig. 2, *I* and *J*). To further confirm the specificity of ICs binding to FcγRIII, we tested the ICs binding to activated Jurkat (Fig. 3*A*), P116 (Fig. 3*B*), both CD4⁺ T-cells, THP-1 (Fig. 3*C*) and Daudi (Fig. 3*D*) that express FcRγII, which also bind to ICs. All these cells demonstrated a population of cells that showed binding to labeled ICs. CD4⁺ cell lines and THP-1 cells demonstrated bimodal IC binding. Although, we are not certain of the underlying mechanism, we speculate that differential binding of the ICs to FcγRIIIa and FcγRIIIb can demonstrate such behavior. The FcγRIIIb binds to ICs with an affinity of $<10^7$ compared with that of FcγRIIIa, which bind with affinity of $\sim 2 \times 10^7\ \text{M}^{-1}$. We further examined whether the IC binding population also bind to anti-FcγRIII antibody (3G8). In all three cell line examined, THP-1, P116, and Jurkat cells, we observed double staining for labeled IC binding with anti-FcγRIII (3G8) antibodies (Fig. 3, *I*, *J*, *K*). These results further establish the specificity of ICs binding to FcRs.

Anti-FcγRIIIa/b Receptor Specific Antibodies Inhibit AHG Binding—Next, we examined whether these antibodies used for cell staining can block the binding of labeled AHG to the activated CD4⁺ T-cells. To set up antibody-specific blocking experiments, we first titrated binding of AHG from concentration of 0.5 to 5 μg/million of activated CD4⁺ T-cells. AHG binding analysis in a flow staining experiment showed a concentration-dependent increase in AHG binding. The percentage of cells that bound to AHG increased from 1.61 to 66.4% and also showed associated increase in mean fluorescent inten-

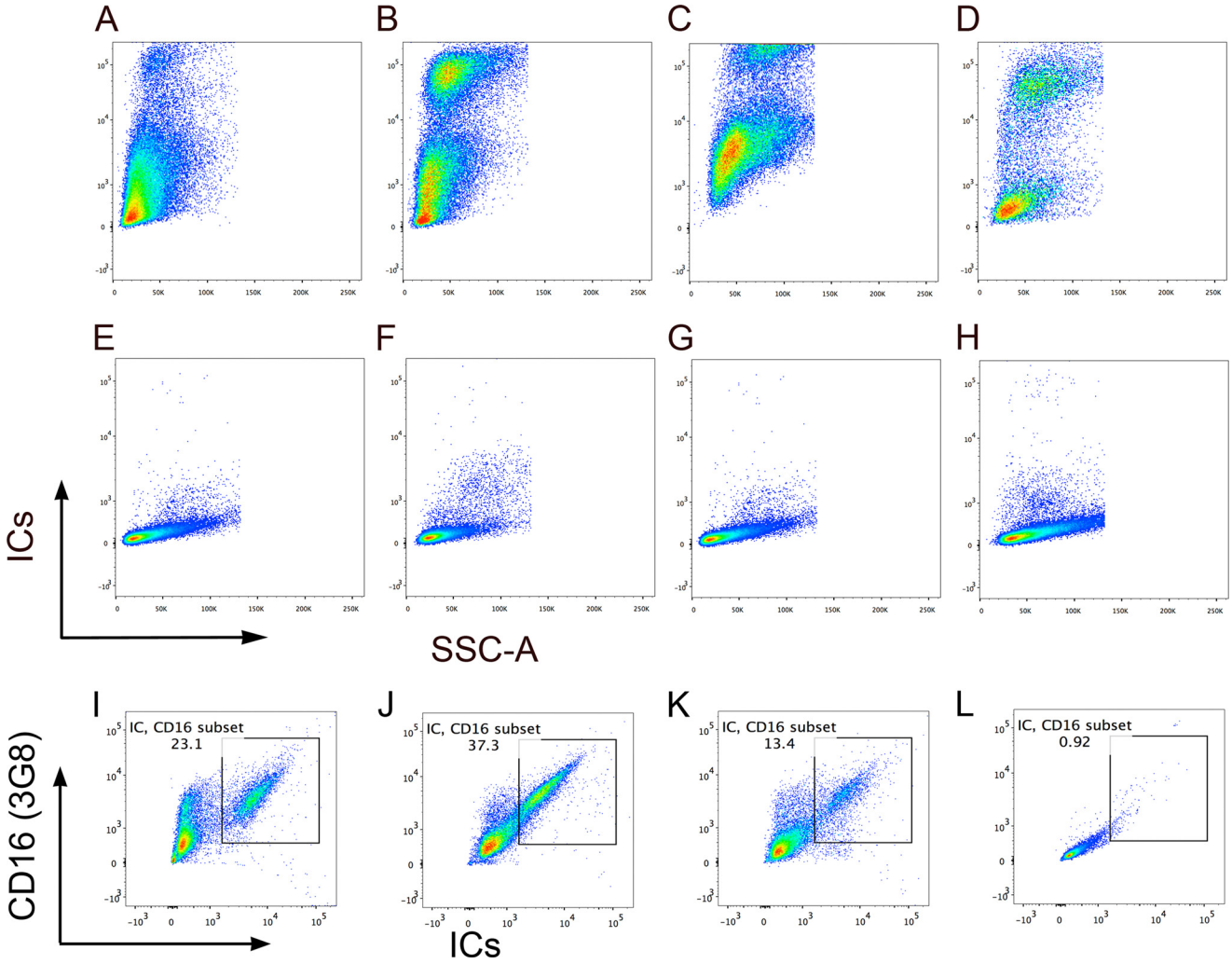

FIGURE 3. **Binding of IC-Alexa-Fluor 488.** Activated CD4$^+$ T-cells Jurkat (*A*), P116 (*B*), and monocytic cells THP-1 (*C*) as well as Daudi B cells (*D*) demonstrate binding to labeled ICs. Unstained Jurkat (*E*), P116 (*F*), THP-1 (*G*), and Daudi (*H*). Dual binding of ICs and anti-CD16 (3G8). THP-1 (*I*), activated P116 (*J*), and activated Jurkat (*K*) and unstained cells (*L*). Cells stained with anti-CD16 also show ICs staining. Data representative of two independent experiments.

sity (MFI) from 16.96 to 193.98 (Fig. 4*A*). A pre-treatment of cells with 5 μg of monoclonal antibody anti-FcγRIIIa/b for 1 h at room temperature inhibited the binding of 2.5 μg of labeled AHG used for each one million cells (Fig. 4*B*). Further increase in the antibody quantity to 10 and 20 μg did not show any further inhibition of the AHG binding (not shown). Under similar conditions isotype control (IgG_2A) at 10 μg did not inhibit AHG binding (Fig. 4*C*). The FcγRIIIa and FcγRIIIb receptor proteins are identical except at the C terminus the FcγRIIIa has additional 21 amino acids that constitute the cytoplasmic tail. This similarity in amino acid sequence has hampered the development of specific reagents for these receptors. Thus, we used the only available antibody that is specific for FcγRIIIb to characterize its presence. The anti-FcγRIIIb antibody used is an affinity-purified goat polyclonal from R&D Systems (Product: AF1597). This antibody also inhibited the AHG binding at a concentration of 5.0 μg (Fig. 4*D*). These results suggest the presence of FcγRIII on activated CD4$^+$ T-cells. The FcγRIIIa and FcγRI signal via common FcR-γ chain, thus we further explored if affinity-purified goat polyclonal anti-FcγRI (R&D systems, Product: AF1257) will block the binding of AHG. The high affinity FcγRI preferentially binds to monomeric immunoglobulin. Affinity-purified polyclonal anti-FcγRI antibody at concentration of 10 and 20 μg of protein showed small amount of inhibition for the AHG binding (Fig. 4*E*). The goat F(ab′)2 fragment used as a control for goat polyclonal at a concentration of 10 μg also did not inhibit AHG binding (Fig. 4*G*). Unstained control cells did not show fluorescence as observed for AHG binding cells, histograms unstained cells (Fig. 4*H*), stained cells (Fig. 4*I*), and scatter overlay (Fig. 4*J*).

Immunoblotting for FcγRIII Proteins—To further characterize the FcγRIII proteins, which bound to AHG and ICs, we generated immunoprecipitates (IPs) using two anti-FcγRIII monoclonal antibodies, clone 245536 and 3G8 from THP-1, Jurkat, and P116 cells. These IPs when probed with polyclonal anti-FcγRIII, showed several protein bands between 20 to 37 kDa, at 53 kDa and at ~75 kDa (Fig. 5*A*). The IPs obtained with clone 245536 antibody in activated Jurkat, CD4$^+$ and P116, all CD4$^+$ T-cells showed more pronounced low molecular weight proteins that were also observed in IPs obtained using 3G8 antibody at low intensity. One of these proteins reacted with anti-ζ chain antibody (not shown). Phosphorylated FcR-γ chains

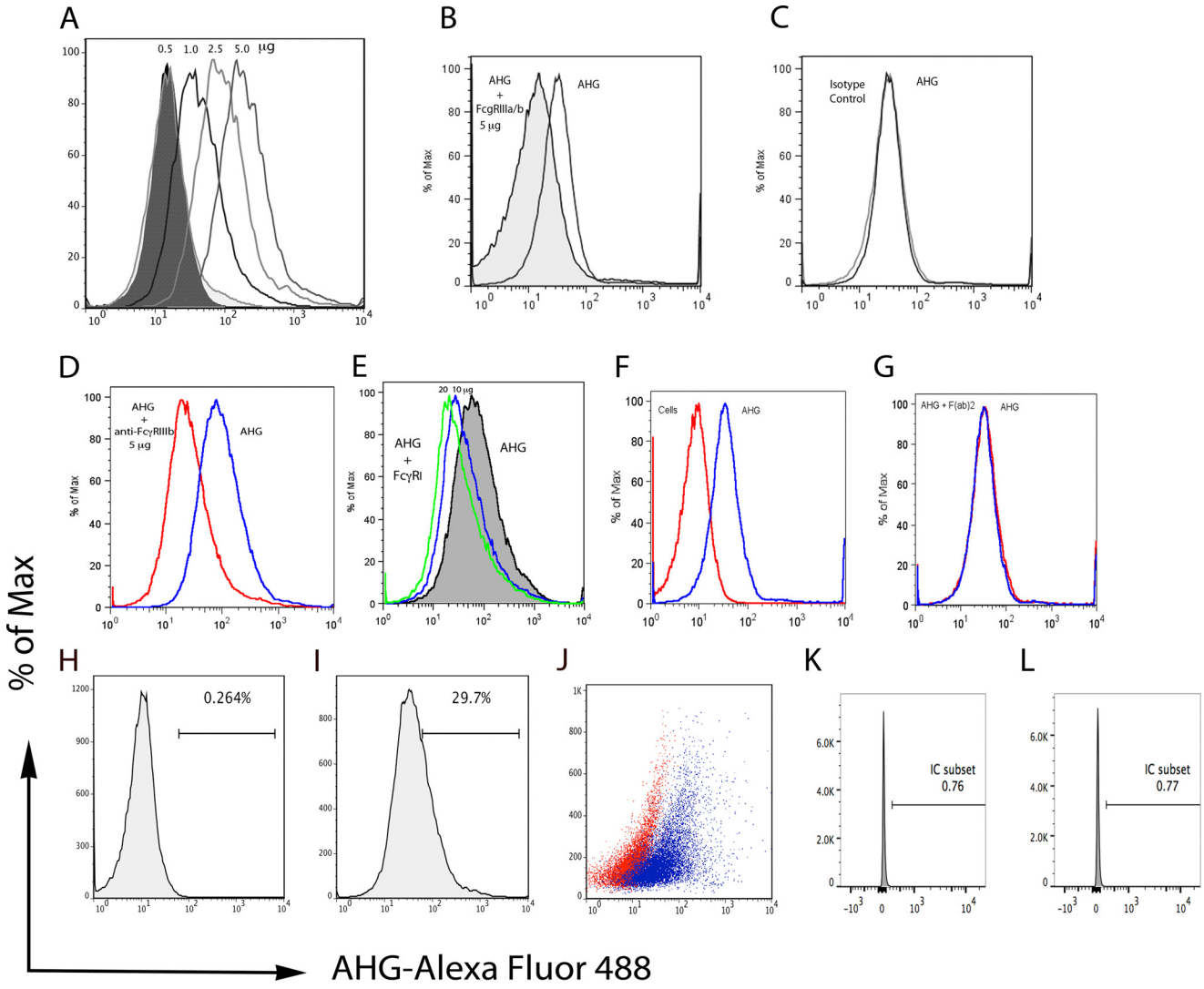

FIGURE 4. **Anti-FcγRIIIa/b antibodies inhibit AHG binding.** *A*, increasing amount of Alexa Fluor-488-AHG from 0.5, 1, 2.5, and 5 μg show linear increase in AHG-binding cells (1.61, 11.20, 29.68, and 66.47%) and increase in MFI (16.96, 56.90, 99.34, and 193.98). *B*, monoclonal anti-FcγRIIIa/b antibody at 5 μg inhibited the AHG binding. Isotype control 10 μg protein did not inhibit AHG binding (*C*). Polyclonal anti-FcγRIIIb at 5 μg inhibits the AHG binding (*red*) (*D*). Polyclonal anti-FcγRI showed slight inhibition (*E*). Unstained cells (*red*) and cells stained with AHG (*blue*) (*F*). Goat F(ab)2 fragment did not inhibit the AHG binding (*G*). Histogram unstained cells (*H*), stained with AHG (*I*), and overlay scatter of H and I (*J*). Unstained cells (*K*) and isotype control (*L*). Data are representative of two independent experiments.

demonstrate molecular mass in this range and forms heterodimers with ζ-chain (28, 29). In direct staining, these proteins did not react to anti-mouse-HRP conjugate. Previously, a 29 and 31 kDa protein along with a broad band at 50–75 kDa that is recognized by anti-CD16 (3G8) antibody has been reported from monocytes (30). Similar size proteins were observed in Jurkat and P116 cells IPs, using anti-CD16 polyclonal antibody (Fig. 5*B*). An inconsistent presence of 40 and 31 kDa proteins were reported in monocytes (30). In addition to 29 kDa protein, human monocytes also express CD16 as a 50–80-kDa protein (31, 32). Human neutrophils show FcγRIII as 29, 33 kDa and a broad band at 50 to 73 kDa (33). In polymorphonuclear cells, 3G8 recognized broad bands at 64–80 kDa, 50–64 kDa and in natural killer cells at 53–59 kDa and 59–65 kDa (34). We observed proteins at these molecular masses in IPs obtained with monoclonal anti-CD16 (3G8, 245536) from CD4$^+$ T-cells that reacted to anti-CD16 polyclonal antibody (Fig. 5, *A* and *B*). Cell lysates analyzed in non-denaturing gels using polyclonal anti-CD16 recognized a protein at ~ 58–60 kDa in Jurkat, P116, and in monocytes obtained from two SLE patients. In THP-1 cells instead a lower mass protein and several faint higher mass proteins were observed (Fig. 5*C*). Human foreskin fibroblast (HFF) and human embryonic kidney cells (293T) cells did not demonstrate the presence of this ~58–60 kDa protein. IPs prepared using anti-CD16 (3G8) antibody after reducing and alkylating with iodoacetamide, revealed several bands from 20 to 37 kDa (33, 35). In addition, a prominent band at ~ 53 kDa was observed (Fig. 5*D*) (36). In control 293T cells less reactive two bands between 20 to 25 kDa were observed. After digestion with *N*-glycanase, majority of the proteins in IPs obtained with anti-CD16 (3G8) appeared as a prominent band at ~21 kDa and a protein at ~ 53 kDa, with a faint band at 40 kDa (Fig. 5*E*). A 21-kDa-protein post *N*-glycanase treatment was reported from polymorhonuclear cells (34). These results further suggest the presence of FcγRIII proteins on CD4$^+$ T-cells.

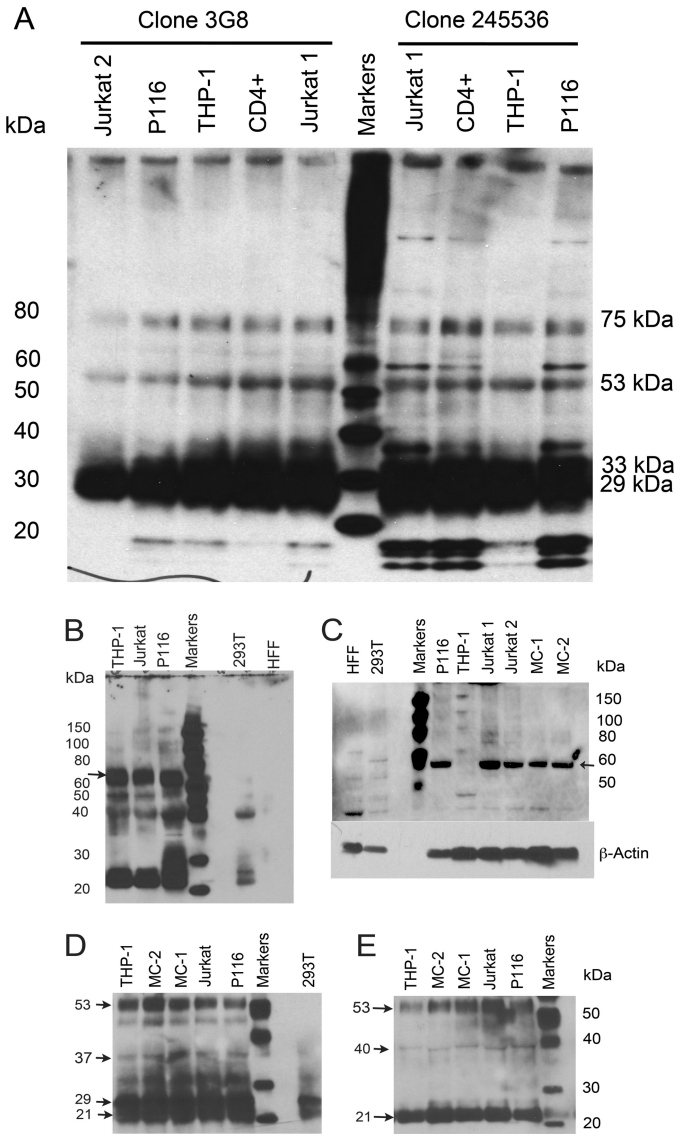

FIGURE 5. **Western blot analysis of immunoprecipitates.** Immunoprecipitates were generated using two monoclonal antibodies, clone 3G8 (*left*) and clone 245536 (*right*). *A*, blots were developed using anti-CD16 polyclonal showed broad-band between 20 to 40 kDa. Additional band at 75 kDa was observed. In CD4⁺ cells, additional band at ~60 kDa was observed in immunoprecipitates with clone 245536. Low molecular weight proteins were observed prominently in IPs with 245536 in CD4⁺ T-cells. A 53-kDa band was observed in all cells. *Lanes left* to *right*, Jurkat 2 (un-stimulated); P116 (un-stimulated); THP-1 (un-stimulated); naïve CD4⁺ T-cells (stimulated with anti-CD3+ICs+C5b9); Jurkat (stimulated with anti-CD3+ICs+C5b-9); Magic Mark XP molecular weight markers; Jurkat 1 (stimulated with anti-CD3+ICs+C5b-9); naïve CD4⁺ T-cells (stimulated with anti-CD3+ICs+C5b-9); THP-1 (un-stimulated) and P116 (stimulated with anti-CD3+ICs+C5b-9). *B*, in CD4+ T-cells and THP-1, a broad protein band at 60–80 kDa and 20–37 kDa along with minor bands at 40 and 50 kDa are observed. *C*, in non-denaturing gels, anti-CD16 polyclonal antibody recognized a protein at ~58–60 kDa in Jurkat, P116 and two monocyte preparations. THP-1 cells showed multiple bands. HFF and 293T cells did not react to 58–60 kDa protein but showed faint bands. HFF showed a low MW reactive protein. *D*, reduction and alkylation of IPs from Jurkat, P116, THP-1, and monocytes showed major multiple bands between 20 to37 kDa and a band at 53 kDa. 293T cells only showed two low intensity bands at 20–25 kDa. *E*, *N*-glycanase digestion of IPs from both monocytes and CD4⁺ T-cells demonstrated a major protein band at 21 kDa. A protein band at 53 kDa with a faint band at 40 kDa was also present.

Activated Human CD4⁺ T-cells Express FCGR3A Transcripts—Having shown that the activated CD4⁺ T-cells show binding to AHG and ICs, also this AHG binding was successfully blocked with anti-FcγRIII antibodies, we next analyzed the presence of *FCGR3A* transcripts in cDNA prepared from anti-CD3+ICs+C5b-9 treated naïve CD4⁺ T-cells. We examined the level of *FCGR3A* RNA transcript expression in human CD4⁺ T-cells at rest or activated with plate-bound anti-CD3+anti-CD28 or anti-CD3+ICs+C5b-9 (IDT assay Hs.PT.49a.15478614g). Expression levels of the RNA transcripts were normalized to anti-CD3 treated cells of each donor. Increased expression of *FCGR3A* transcripts, ranging from 4.4–23-fold was observed in all the six donors analyzed in response to anti-CD3+ICs+C5b-9 treatment (Fig. 6*A*). Induced expression of *FCGR3A* transcripts at lower level compared with anti-CD3+ICs+C5b-9 stimulation was also observed in three of six donors analyzed from anti-CD3+anti-CD28 stimulation. The relative amount of expression varied between the two types of stimulation (Fig. 6*A*). We further analyzed the time course for expression of *FCGR3A* gene transcripts. This data showed that the *FCGR3A* gene transcripts appeared as early as day 4 post-stimulation in anti-CD3+anti-CD28 treated cells and by day 30 *FCGR3A* transcripts returned to baseline levels (Fig. 6*B*). Maximum expression of *FCGR3A* transcripts in anti-CD3+ICs+C5b-9-treated cells was observed on day 9. In anti-CD3+anti-CD28-treated cells *FCGR3A* expression peaked earlier compared with anti-CD3+ICs+C5b-9 treatment. Visual microscopic examination also showed early colony formation and expansion of cells from anti-CD3+anti-CD28 treatment. Additional analysis of nine donors for *FCGR3A* expression without stimulation at zero time did not show any significant difference in *FCGR3A* transcripts (Fig. 6*C*). A less than 2-fold variation was observed among these donors using a random donor for *FCGR3A* expression as a control. The gene expression assay obtained from IDT is designed to recognize a *FCGR3A* gene variant. Our analysis showed that the primers used in this assay might recognize both *FCGR3A* as well as *FCGR3B* gene product. However staining with antibodies suggests a predominant expression of FcγRIIIa, which signal via FcR-γ chain (Fig. 1*F*).

DNA Sequencing of PCR-amplified Product Confirm FCGR3 Gene—Once we established *FCGR3A* transcripts in the activated CD4⁺ T-cells, we further confirmed their identity by DNA sequencing. To accomplish this, we designed primers based on gene ID NM-001127596.1 (GI: 189083841). In PCR amplification, these primers generated an appropriate size 330-bp fragment from activated Jurkat, naïve CD4⁺ T-cells and pooled lymphocytes (Fig. 7*A*, *left panel*). Thereafter, using nested M13-FCGR3 primers we re-amplified this product (367 bp) and sequenced it with M13 primers from both sides (Fig. 7*A*, *right panel*). The nucleotide sequence obtained from dideoxy sequencing of this fragment upon blast analysis (NCBI) confirmed it to be a *FCGR3A* gene product that aligned to nucleotides 535 to 831 of gi 1890838441 ref NM_00127596.1 (Fig. 7*B*). The confirmed sequence covered exons 4 and 5 (Fig. 7*C*). This sequence also aligned to the 434 to 732 nucleotide of gi 46430439 ref AJ581669.1 of *FCGR3B* gene. Thus, these results further confirmed the presence of *FCGR3* gene transcripts in activated CD4⁺ T-cells. In addition, primers used to establish the presence of *FCGR3B*, a 242-bp fragment in baso-

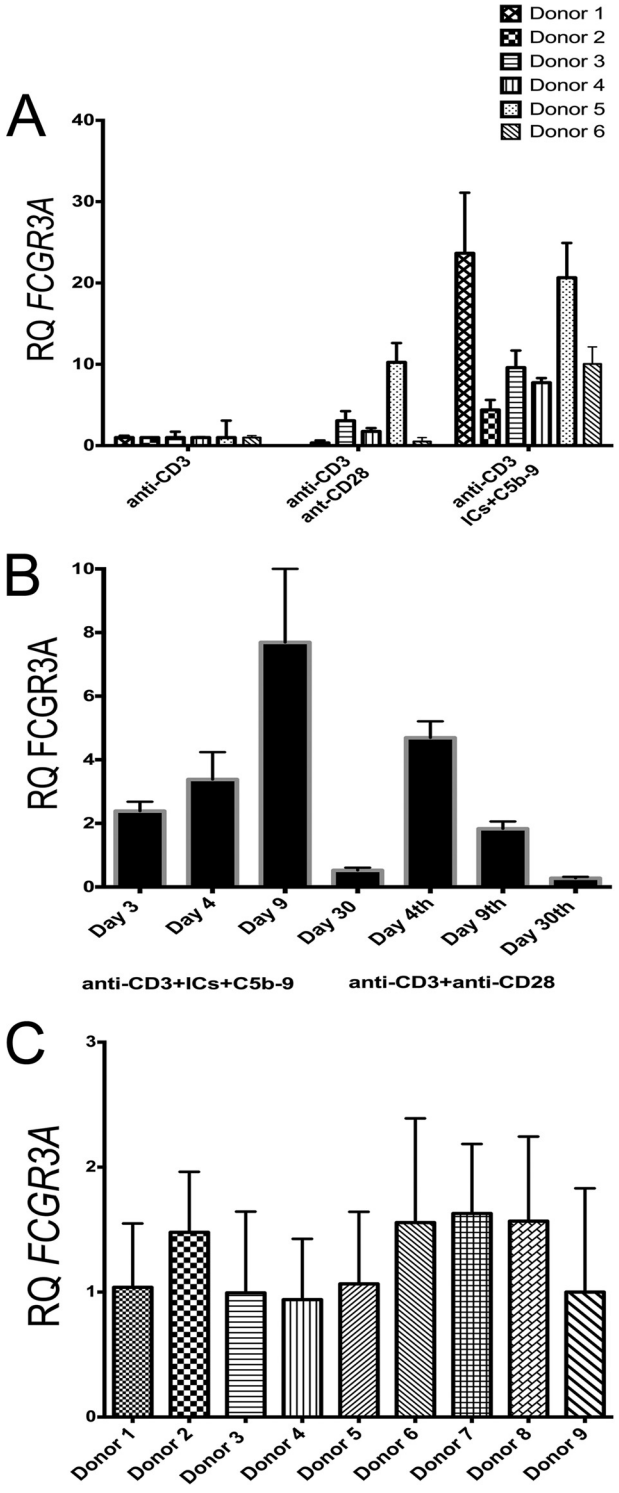

FIGURE 6. **qRT-PCR analysis of *FCGR3A* gene transcripts.** *FCGR3A* gene is expressed in activated CD4$^+$ T-cells. *A*, all six donors analyzed showed an increase in the *FCGR3A* gene transcript from anti-CD3+ICs+C5b-9 activation and 3 of 6 from anti-CD3+antiCD-28 activation on day nine. Data are normalized with anti-CD3 for each donor population. *B*, time course analysis for *FCFGR3A* transcripts in CD4$^+$ T-cells show maximum expression on day 9 with anti-CD3+ICs+C5b-9 and on day 4 with anti-CD3+anti-CD28 activation. Data are representative of two independent experiments. *C*, nine donors analyzed for the relative quantities (RQ) of *FCGR3A* transcripts in CD4$^+$CD45RA$^+$ T-cells (at 0 time point). Donors 2, 6, 7, and 8 showed relatively small increase. *FCGR3A* normalized with endogenous control *GAPDH*. *FCGR3A* in all donors was normalized using the donor 1 transcripts.

phils also successfully amplified an appropriate size a 242-bp DNA fragment (not shown) (37).

Production of IFN-γ in the Presence of IL-12 Cytokine—To determine whether the induced expression of FcγRIIIa on CD4$^+$ T-cells has a role in T-cell-mediated immune responses, we evaluated IFN-γ production. IFN-γ is a pleiotropic cytokine, which is also a marker of T_H1 response. T_H1 response is commonly observed in autoimmune pathology (38, 39). Thus, we examined both production of IFN-γ and T-bet expression, a transcription factor that regulates IFN-γ production during T_H1 response (39). Both FcγRIIIa and FcγRIIIb are capable of binding to ICs. FcγRIIIa mediates antibody-dependent cellular cytotoxicity (ADCC), and phagocytosis, contrary FcγRIIIb is not capable of these functions and only acts as a trap for ICs. FcγRIIIa signals via activating FcR-γ chain that couples to activation and this signal drives IFN-γ production in macrophages (40). In T-cells, FcR-γ chain is present as a heterodimer with ζ-chain in the T-cell receptor (TCR).

We analyzed 12 subjects in three independent experiments for IFN-γ production and T-bet expression. In a donor shown, the cells treated with anti-CD3+anti-CD28 showed 9.6% IFN-γ$^+$T-bet$^+$ cells, while anti-CD3+ICs+C5b-9 treated group showed 24% of double positive cells (Fig. 8, *A* and *B*). A distinct higher amount of IFN-γ production in cells treated with anti-CD3+ICs+C5b-9 was observed compared with anti-CD3+anti-CD28 treatment in this donor (Fig. 8, *A* and *B*). Substantial and significant increase in the expression for IFN-γ and T-bet was observed in 10 subjects in response to treatment with anti-CD3+ICs+C5b-9 (Fig. 8, *C* and *D*). Cells from two donors did not respond to any stimulation. Combined analysis of ten donors showed an increase in IFN-γ$^+$T-bet$^+$ cells from 6.37 ± 1.33 (anti-CD3) to 20.4 ± 3.48 (anti-CD3+ICs+C5b-9) and 9.48 ± 2.74 (anti-CD3+anti-CD28). This increase was statistically significant at a p value of 0.0014 for anti-CD3+ICs+C5b-9 treated cells compared with anti-CD3 treatment (Fig. 8*D*). Donors 8, 9, and 10 showed higher percentage of IFN-γ$^+$T-bet$^+$ cells from anti-CD3+anti-CD28 treatment (Fig. 7*C*). When compared with cells alone the increase in IFN-γ$^+$T-bet$^+$ population was more pronounced and statistically significant with both stimulations. An increase from 2.43 ± 0.81 (cells) to 20.49 ± 3.48 (anti-CD3+ICs+C5b-9) and 9.49 ± 2.74 (anti-CD3+anti-CD28) was observed, which were statistically significant at a p value of 0.0001 and 0.0239, respectively. We observed a population that produced high amount of IFN-γ and a population that produced moderate amount of IFN-γ (Fig. 8). These results thus suggest a role for FcγRIIIa signaling in the production of IFN-γ in peripheral CD4$^+$ T-cells. The analysis of the gene transcripts that encode for IFN-γ (*ifng*) and T-bet (*Tbx21*) showed increase in anti-CD3+ICs+C5b-9 treated cells (Fig. 9, *A* and *B*). In the five donors analyzed, *ifng* transcripts showed an increase from 1.8 to 6.49-fold (Fig. 9*A*). An increase in *Tbx21* transcripts up to 2.8-fold was observed. Cells treated with anti-CD3+anti-CD28 also showed increase in both gene transcripts, except donor 3, which did not express *Tbx21* (Fig. 9*B*). FcγRIIIa from IC ligation signals via ITAM by recruiting common FcR-γ chain. This suggests a role for FcγRIIIa in IFN-γ production. These results further assert not only the presence of signaling FcγRIIIa receptor on activated

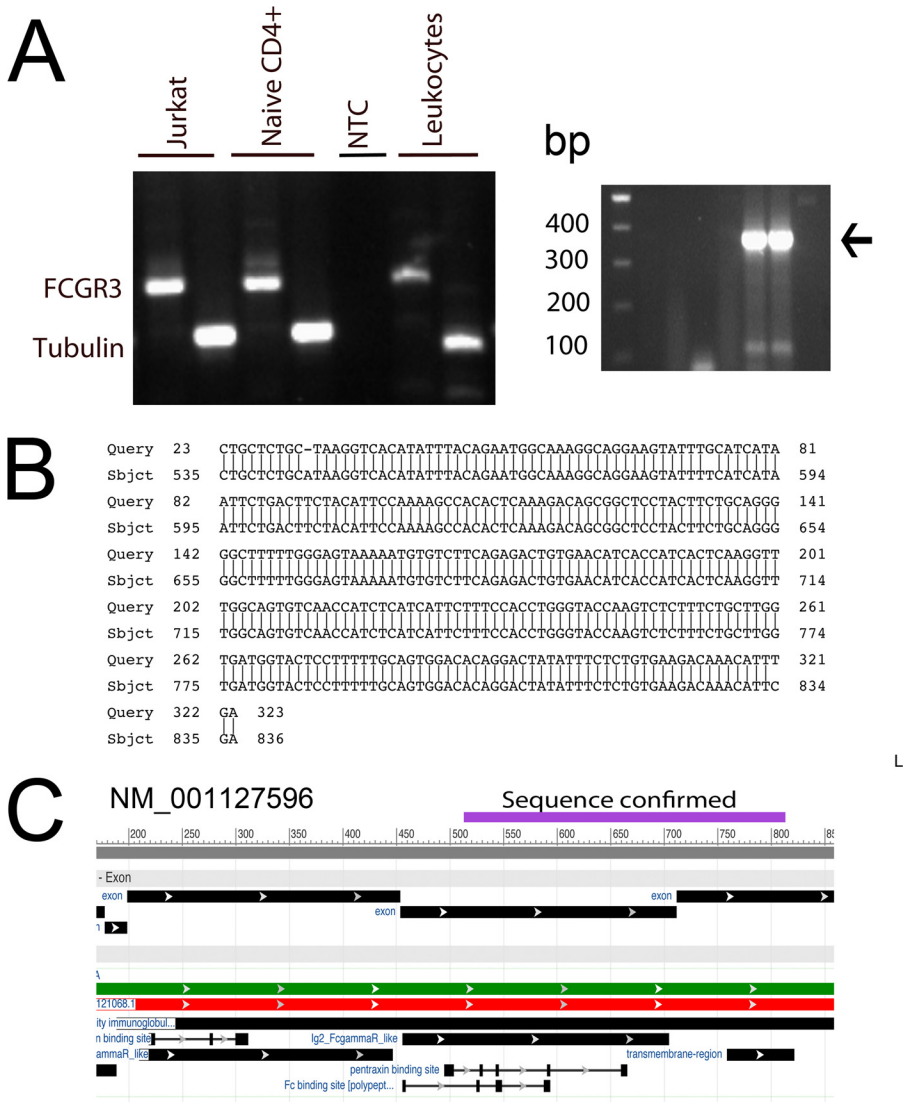

FIGURE 7. **Sequencing of amplified *FCGR3* cDNA fragment.** RT-PCR for FCGR3 transcripts from activated Jurkat, naïve CD4$^+$, and leukocytes show an amplification product size of 330 (*A*, *left panel*). *NTC*, no template-control. Re-amplified product with nested M13-FCGR3 primers generated a 367 bp DNA fragment, which was sequenced with M13 primers (*A*, *right panel*). *B*, dideoxy sequence obtained aligned to NM_001127596. *C*, sequenced fragment aligned to cDNA coding for exons 4 and 5.

CD4$^+$ T-cells, but also a function for FcγRIIIa in T-cell response.

Subsets of Mouse CD4$^+$ T-cells from Two Different Autoimmune Models Bind to Labeled ICs—To examine whether the activated CD4$^+$ T-cells population is also present in disease state, we examined the binding of labeled ICs in two mouse models of autoimmunity. First, we examined CD4$^+$ T-cells from the K/BxN arthritis mouse model. ICs and auto reactive CD4$^+$ T-cells causes joint disease in this mouse model, both of which target the glucose-6-phosphoisomerase enzyme (22). Flow analysis for IC binding showed that a subset of activated CD4$^+$ T-cells from K/BxN mice demonstrated increased binding for the labeled ICs. A 4-fold increase in IC binding (from 1.7 to 7.3%) was observed in CD4$^+$ T-cells from K/BxN compared with KRN control mice. Furthermore, a 3-fold increase (from 13 to 31%) in the binding of labeled AHG by CD4$^+$ T-cells from K/BxN mice compared with control KRN mice (not shown). Next, we examined CD4$^+$ T-cells from the TxA23 mouse model of Autoimmune Gastritis (23). As in the human disease, CD4$^+$ T-cells and autoantibodies that target the H+/K$^+$ ATPase enzyme expressed in the stomach cause disease in mouse. Increased IC binding of 9.3% in CD4$^+$ T cell population was also observed in autoimmune gastritis model (TxA23) compared with 3.4% binding in BALB/c control group (Fig. 10) Increase in ICs binding was statistically significant in both diseases. Together these data demonstrate an increase in IC binding CD4$^+$ T-cell population in two separate mouse models of autoimmunity.

The binding of AHG and ICs, staining and inhibition of AHG binding along with qRT-PCR for FcγRIIIa RNA transcripts and DNA sequencing of amplified transcripts, thus confirms the presence of this FcγRIII receptor in a subset of activated CD4$^+$ T-cells.

DISCUSSION

FcRs interact with the monomeric immunoglobulin's and ICs to trigger cell specific functions (7). In this report, we show that the activated peripheral CD4$^+$ T-cells express low affinity

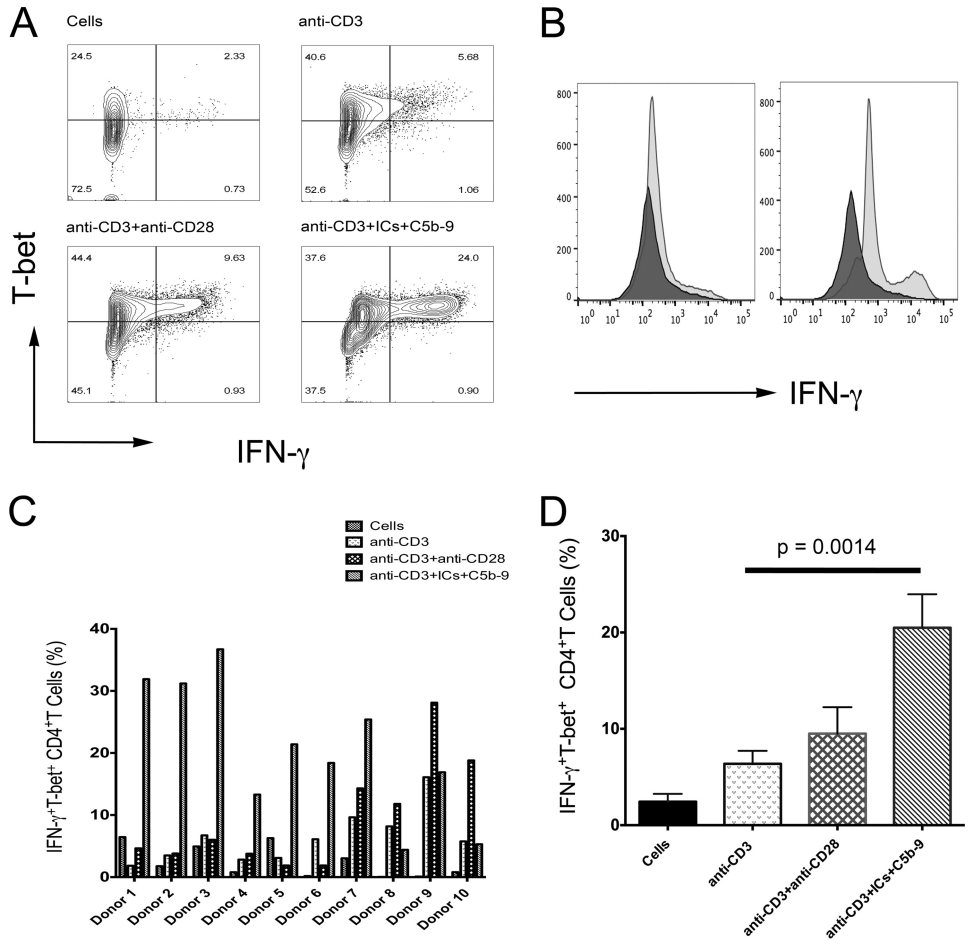

FIGURE 8. **ICs and C5b-9 trigger IFN-γ production.** Flow analysis for IFN-γ production and T-bet expression in CD4$^+$ gated cells. *A*, one of the ten responding donor showed 24% IFN-γ$^+$T-bet$^+$ cells from anti-CD3+ICs+C5b-9 activation compared with 9.63% in response to anti-CD3+anti-CD28 activation. *B*, histogram comparing IFN-γ production from anti-CD3+anti-CD28 treatment *versus* anti-CD3+ICs+C5b-9 compared with anti-CD3 treated population. *C*, percentage of cells expressing IFN-γ and T-bet in 10 donors of total 12 analyzed. 7 donors showed high population of IFN-γ$^+$T-bet$^+$ in response to anti-CD3+ICs+C5b-9 and 3 donors (8, 9, and 10) from anti-CD3+anti-CD28 treatment (*D*) Combined analysis for IFN-γ$^+$T-bet$^+$ showed statistically significant increase in anti-CD3+ICs+C5b-9 treated cells at a *p* value of 0.0014 compared with anti-CD3 treated.

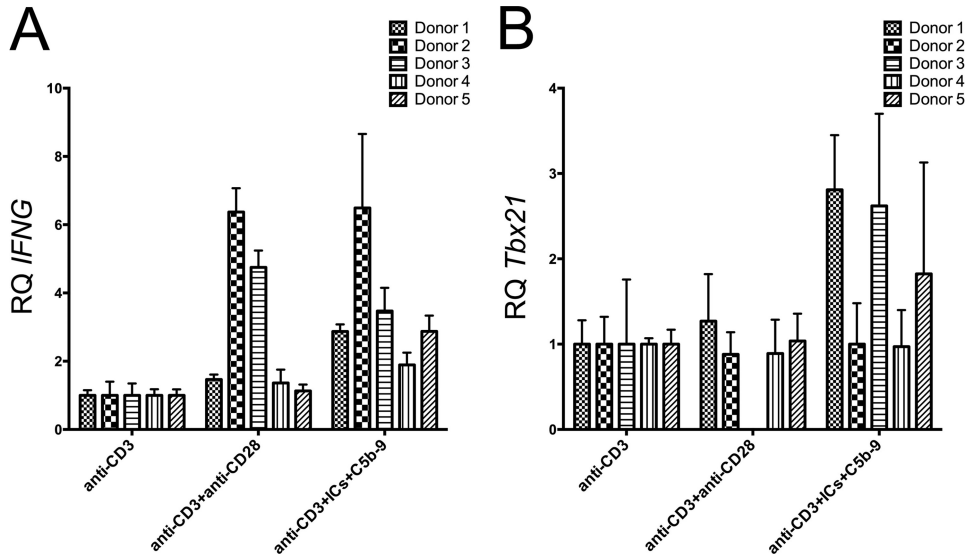

FIGURE 9. **Expression for *Ifng/Tbx21* gene in activated CD4$^+$ T-cells.** qRT-PCR analysis for *ifng* (*A*) *and Tbx21* (*B*) gene transcripts in five donors with two treatments. All of the five donors analyzed demonstrated an increase in *ifng* transcripts from 1.8–6.8-fold in the anti-CD3+ICs+C5b-9 treated group and no change to 6.37-fold in the anti-CD3+anti-CD28-treated group. For *Tbx21* transcripts demonstrated an increase from no change to 2.8-fold, and no change to 1.4-fold increase was observed in anti-CD3+ICs+C5b-9 and anti-CD3+anti-CD28, respectively. Donor 3 did not express *Tbx21* from anti-CD3+anti-CD28 treatment.

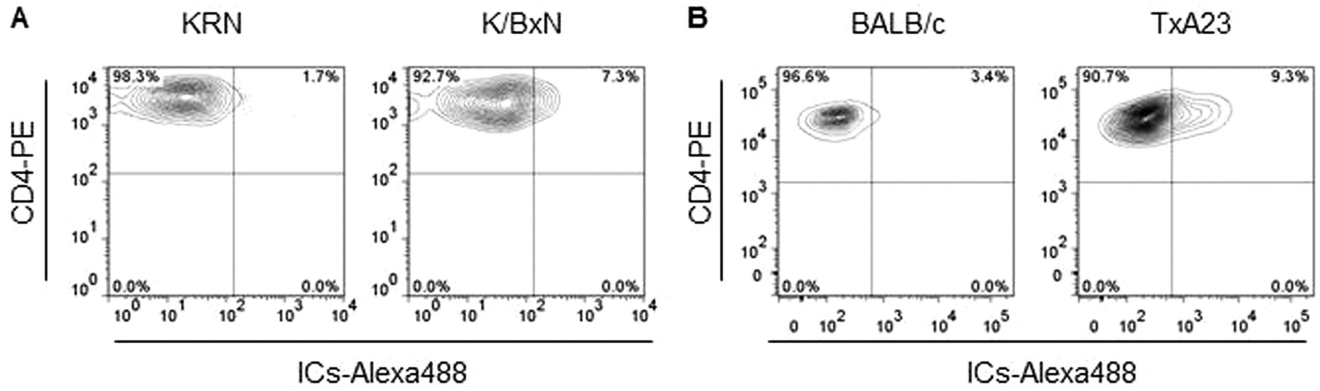

FIGURE 10. **Surface binding of ICs to CD4⁺ T cells from two different mouse models of autoimmunity.** *A*, increased ICs binding to CD4⁺ T-cells from KRN mice crossed to NOD mice (K/BxN), a well-established mouse model of autoimmune arthritis, but not to CD4⁺ T-cells from control KRN mice. Data is representative of an analysis that included 6 mice per group. *B*, ICs binding to CD4⁺ T-cells from TxA23 mice, a well-established mouse model of Autoimmune Gastritis, but not to CD4⁺ T-cells from control (BALB/c) mice. Data are representative of an analysis that included 5 mice per group.

FcγRIIIa receptor that upon ligation with ICs in the presence of IL2/IL-12 generate a strong IFN-γ producing subset. FcRs are widely expressed by immune cells and play a critical role in many immune -mediated responses. Despite some early reports for the presence of FcRs on CD4⁺ T-cells, their role in T-cell mediated immune responses has been largely ignored (15, 17, 41, 42). We observed a co-staining of ICs with the CD3 complex on CD4⁺ T-cell membrane and observed T-cell activation from ICs+C5b-9 treatment (24). In CD4⁺ T-cells, engagement of the FcRs by ICs led to the phosphorylation of FcR-γ chain, which co-localized with phosphorylated Syk kinase (43). In the present study, we show activation induced expression of FcγRIIIa in a subset of activated CD4⁺ T-cells that upon ligation from ICs led to the development of a cell phenotype that produced high amounts of IFN-γ and expressed T-bet. Another subset produced moderate amount of IFN-γ (Fig. 8, *A* and *B*). We speculate that this population was produced by the secondary activation from the first wave of IFN-γ and T-bet expression resulting from IC ligation. During T_H1 response, IFN-γ and T-bet expression is observed in two waves (44). Although the precise mechanism that derive the IFN-γ production from ICs+C5b-9 stimulation is not clearly understood, we speculate the possible involvement of DAP-12- Syk-CARD9 pathway. A role for Syk in the production of IFN-γ from CD16 ligation in natural killer has been reported (45). We observed decrease in ICs binding population in a secondary stimulation experiment, which coincided with the increase of IFN-γ population, suggesting FcγRIII utilization.[3] The possibility do exists that the other secondary mediators may be involved. Nonetheless production of IFN-γ by ICs+C5b-9 is an important event.

We observed up to twenty-five percent of cell population that expressed FcγRIII. A previous study has also demonstrated IgG binding to as much as 20% of T cells (46). Since most of commercial IgG preparations (typically the Cohn fraction V) are contaminated with the aggregated globulin, we believe that in this study aggregated IgG contributed to the observed binding (46). In the mononuclear leukocytes, activation of enriched T lymphocytes also demonstrate an increase in the number of CD3⁺ FcγRIIIa⁺ cells on day 4 poststimulation with immobilized human IgG (42). Furthermore, PHA stimulation showed 4–10-fold increase in FcγRIII⁺ population within CD3⁺CD8⁺ population (42). A total of 3 to 5% CD4⁺ T-cells expressed CD16 and this population did not increase in response to immobilized IgG (42). These previous studies demonstrate the presence of low affinity FcRs on T lymphocytes. In mouse, yet another study showed that the mouse Thy-1⁺ thymocytes express FcγR between 13 and 17 days of fetal development (47). In this report, we define two more activation signals that induce the expression of FcγRIII on peripheral human naïve CD4⁺ T-cells. The percentage of FcR⁺-bearing cells and timing of expression observed by us is also in agreement to these previous studies (Figs. 1 and 2). With repeated *in vitro* activation as high as a ≈50% cells demonstrate IC binding. Our result along with these previous studies are in contrast to several recent reports that argue for the lack of expression of FcRs on CD4⁺ T lymphocytes (4, 5, 7, 9, 10, 48). We believe that the lack of good antibodies against human FcRs and lack of proper reagents to analyze the expression of FcγRIII on activated CD4⁺ T-cells contributed to the non-recognition of these receptors on CD4⁺ T lymphocytes by several groups.

In addition to human studies that point to the presence of low affinity FcRs on CD4⁺ lymphocytes, previous literature has also established binding of aggregated mouse IgG to murine thymocytes and T cells (49). We examined two disease mouse models for an increase in the binding of ICs to CD4⁺ T-cells. In both of these diseases, we observed increased CD4⁺IC⁺ population compared with non-disease mouse (Fig. 10). Increased IC binding was also observed directly in the CD4⁺ population in SLE patients (43). The IC binding and staining with receptor specific antibodies demonstrated IC co-localization with the receptors (Fig. 1*E* and supplemental Fig. S1). The staining pattern observed suggest receptor capping (Fig. 1*E*). The binding of aggregated mouse globulin appeared as fluorescent speckles incorporated into the cell beneath the membrane (49). A similar staining pattern of ICs binding to the human CD4⁺ T cells was observed (24).

ICs and C5b-9 are common immune reactants of humoral and innate immune responses and are elevated during disease pathologies such as autoimmunity, infections, and cancers. Both ICs and C5b-9 are present within the immune deposit,

[3] A. Chauhan, unpublished observation.

which occurs in vascular sites in conditions such as lupus nephritis and arthritic synovium (50, 51). Thus those naïve CD4$^+$ T-cells that will come in contact with immune deposits will trigger their differentiation into CD4$^+$FcγRIIIa$^+$IFN-γ^{high} population resulting in high IFN-γ in localized tissue. This excessive production of IFN-γ will lead to the enhanced antigen presentation from increased MHC expression (52). Thus in tissue with immune deposits, activation and differentiation of naïve CD4$^+$ T-cells could modulate local immune responses. This will be important in autoimmune diseases where tissue damage often occurs at vascular sites along with the formation of immune deposits such as kidney. IFN-γ is an important mediator of immunity and inflammation that signals via Jak-STAT1 signaling pathway and amplifies T_H1 response, while suppressing other responses such as T_H2 and T_H17 (53). Thus, ICs-mediated production of IFN-γ could generate a T_H1 bias in the inflammatory tissue with immune deposits. T-bet-deficient cells produce small amount of IFN-γ and fails to mount effective T_H1 response (54). We observed a strong IFN-γ production in a subset of CD4$^+$ T-cells, which suggest that ICs+C5b-9 mediated early IFN-γ may be a protective mechanism employed by host to prevent infection in inflammatory tissue.

The activation-induced expression of FcγRIIIa raises two important questions: 1. Which signaling pathway do these receptors trigger in CD4$^+$ T-cell? 2. In what adaptive responses FcRs play a role? In B cells, FcR-γ chain phosphorylation triggers Syk-PLC-γ2 signaling that results in cell activation (55). Syk-mediated signaling trigger IFN-γ production in macrophages. Thus it is possible that ICs trigger IFN-γ production via Syk signaling in activated CD4$^+$ T-cells (40). SLE is a disease associated with the formation of DNA/RNA containing ICs and hyperactive T cells that also demonstrate activation of Syk (56). It is likely that ICs mediated IFN-γ production in CD4$^+$ T-cells also require Syk activation (Fig. 8). In B cells, FcγRs regulate cellular responses by co-engaging with other membrane receptors *i.e.* complement or B cell receptor in B cells (48, 57). This further raises a question whether FcRs in CD4$^+$ T-cells will exercise similar regulatory role during the disease response by co-engaging TCR (24). In such a scenario, FcγRIIIa mediated activating signal may subvert immune down-regulation during the contraction phase of immunity (24). A role for activating Fc-γ receptors in therapies targeting T cell antigen such as CTLA-4 and GITR is suggested (58, 59). Activation induced expression of FcγRIIIa may influence the outcome of therapies targeting T cell antigens.

In conclusion, we show that upon activation, a subset of the CD4$^+$ T-cell population express FcγRIII both as RNA transcript and protein. Engagement of these receptors by ICs triggers production of high levels of IFN-γ. We also demonstrate limited expression of FcγRIIIb, however their role in T-cell responses is not clear. The presence of FcRs on activated CD4$^+$ T-cells will be an important regulator of immune homeostasis. FcγRIIIa may be the critical link among ICs and hyper-activated T-cell phenotypes observed in SLE. Thus, further exploring FcγRs role in T-cell physiology is critical for understanding of immune homeostasis and autoimmune pathology. These results may have wider implication in diseases such as cancers and not limited to autoimmunity (58, 59). Our results re-emphasize for further exploration of the role of FcRs in T-cell physiology.

Acknowledgments—We thank Thanh-Long Nguyen and Kyle Wolf for careful reading and suggestions.

REFERENCES

1. Nimmerjahn, F. (2006) Activating and inhibitory FcgammaRs in autoimmune disorders. *Springer Sem. Immunopathol.* **28,** 305–319
2. Takai, T. (2005) Fc receptors and their role in immune regulation and autoimmunity. *J. Clin. Immunol.* **25,** 1–18
3. Willcocks, L. C., Lyons, P. A., Clatworthy, M. R., Robinson, J. I., Yang, W., Newland, S. A., Plagnol, V., McGovern, N. N., Condliffe, A. M., Chilvers, E. R., Adu, D., Jolly, E. C., Watts, R., Lau, Y. L., Morgan, A. W., Nash, G., and Smith, K. G. (2008) Copy number of FCGR3B, which is associated with systemic lupus erythematosus, correlates with protein expression and immune complex uptake. *J. Exp. Med.* **205,** 1573–1582
4. Takai, T. (2002) Roles of Fc receptors in autoimmunity. *Nature Reviews. Immunology* **2,** 580–592
5. Nimmerjahn, F., and Ravetch, J. V. (2006) Fcgamma receptors: old friends and new family members. *Immunity* **24,** 19–28
6. Ravetch, J. V., and Clynes, R. A. (1998) Divergent roles for Fc receptors and complement *in vivo*. *Annu. Rev. Immunol.* **16,** 421–432
7. Nimmerjahn, F., and Ravetch, J. V. (2008) Fcγ receptors as regulators of immune responses. *Nature Reviews Immunology* **8,** 34–47
8. Salmon, J. E., and Pricop, L. (2001) Human receptors for immunoglobulin G: key elements in the pathogenesis of rheumatic disease. *Arthr. Rheum.* **44,** 739–750
9. Smith, K. G., and Clatworthy, M. R. (2010) FcγRIIB in autoimmunity and infection: evolutionary and therapeutic implications. *Nature Reviews Immunology* **10,** 328–343
10. Hogarth, P. M., and Pietersz, G. A. (2012) Fc receptor-targeted therapies for the treatment of inflammation, cancer and beyond. *Nature Reviews. Drug Discovery* **11,** 311–331
11. Durandy, A., Kaveri, S. V., Kuijpers, T. W., Basta, M., Miescher, S., Ravetch, J. V., and Rieben, R. (2009) Intravenous immunoglobulins–understanding properties and mechanisms. *Clin. Exp. Immunol.* **158,** 2–13
12. Clynes, R. (2007) IVIG therapy: interfering with interferon-γ. *Immunity* **26,** 4–6
13. Lanier, L. L., Kipps, T. J., and Phillips, J. H. (1985) Functional properties of a unique subset of cytotoxic CD3+ T lymphocytes that express Fc receptors for IgG (CD16/Leu-11 antigen). *J. Exp. Med.* **162,** 2089–2106
14. Sandor, M., and Lynch, R. G. (1993) Lymphocyte Fc receptors: the special case of T cells. *Immunology Today* **14,** 227–231
15. Moretta, L., Ferrarini, M., Mingari, M. C., Moretta, A., and Webb, S. R. (1976) Subpopulations of human T cells identified by receptors for immunoglobulins and mitogen responsiveness. *J. Immunol.* **117,** 2171–2174
16. Moretta, L., Mingari, M. C., Moretta, A., and Fauci, A. S. (1982) Human lymphocyte surface markers. *Sem. Hematol.* **19,** 273–284
17. Sandor, M., Gajewski, T., Thorson, J., Kemp, J. D., Fitch, F. W., and Lynch, R. G. (1990) CD4+ murine T cell clones that express high levels of immunoglobulin binding belong to the interleukin 4-producing T helper cell type 2 subset. *J. Exp. Med.* **171,** 2171–2176
18. Qian, D., Sperling, A. I., Lancki, D. W., Tatsumi, Y., Barrett, T. A., Bluestone, J. A., and Fitch, F. W. (1993) The γ chain of the high-affinity receptor for IgE is a major functional subunit of the T-cell antigen receptor complex in γδ T lymphocytes. *Proc. Natl. Acad. Sci. U. S. A.* **90,** 11875–11879
19. Shores, E., Flamand, V., Tran, T., Grinberg, A., Kinet, J. P., and Love, P. E. (1997) Fc ϵRIγ can support T cell development and function in mice lacking endogenous TCR ζ-chain. *J. Immunol.* **159,** 222–230
20. Liu, C. P., Lin, W. J., Huang, M., Kappler, J. W., and Marrack, P. (1997) Development and function of T cells in T cell antigen receptor/CD3ζ knockout mice reconstituted with Fcϵ RIγ. *Proc. Natl. Acad. Sci. U. S. A.* **94,** 616–621
21. Tan, E. M., Cohen, A. S., Fries, J. F., Masi, A. T., McShane, D. J., Rothfield,

N. F., Schaller, J. G., Talal, N., and Winchester, R. J. (1982) The 1982 revised criteria for the classification of systemic lupus erythematosus. *Arthritis Rheumatism* **25,** 1271–1277
22. Monach, P., Hattori, K., Huang, H., Hyatt, E., Morse, J., Nguyen, L., Ortiz-Lopez, A., Wu, H. J., Mathis, D., and Benoist, C. (2007) The K/BxN mouse model of inflammatory arthritis: theory and practice. *Methods Mol. Med.* **136,** 269–282
23. McHugh, R. S., Shevach, E. M., Margulies, D. H., and Natarajan, K. (2001) A T cell receptor transgenic model of severe, spontaneous organ-specific autoimmunity. *Eur. J. Immunol.* **31,** 2094–2103
24. Chauhan, A. K., and Moore, T. L. (2011) T cell activation by terminal complex of complement and immune complexes. *J. Biol. Chem.* **286,** 38627–38637
25. Ptak, W., Paliwal, V., Bryniarski, K., Ptak, M., and Askenase, P. W. (1998) Aggregated immunoglobulin protects immune T cells from suppression: dependence on isotype, Fc portion, and macrophage FcγR. *Scandinavian J. Immunol.* **47,** 136–145
26. Chauhan, A. K., and Moore, T. L. (2006) Presence of plasma complement regulatory proteins clusterin (Apo J) and vitronectin (S40) on circulating immune complexes (CIC). *Clin. Exp. Immunol.* **145,** 398–406
27. Low, J. M., Chauhan, A. K., Gibson, D. S., Zhu, M., Chen, S., Rooney, M. E., Ombrello, M. J., and Moore, T. L. (2009) Proteomic analysis of circulating immune complexes in juvenile idiopathic arthritis reveals disease-associated proteins. *Proteomics Clinical Applications* **3,** 829–840
28. Gibbins, J., Asselin, J., Farndale, R., Barnes, M., Law, C. L., and Watson, S. P. (1996) Tyrosine phosphorylation of the Fc receptor γ-chain in collagen-stimulated platelets. *J. Biol. Chem.* **271,** 18095–18099
29. Orloff, D. G., Ra, C. S., Frank, S. J., Klausner, R. D., and Kinet, J. P. (1990) Family of disulphide-linked dimers containing the ζ and η chains of the T-cell receptor and the γ chain of Fc receptors. *Nature* **347,** 189–191
30. Clarkson, S. B., and Ory, P. A. (1988) CD16. Developmentally regulated IgG Fc receptors on cultured human monocytes. *J. Exp. Med.* **167,** 408–420
31. van de Winkel, J. G., and Capel, P. J. (1993) Human IgG Fc receptor heterogeneity: molecular aspects and clinical implications. *Immunology Today* **14,** 215–221
32. Stroncek, D. F., Skubitz, K. M., Plachta, L. B., Shankar, R. A., Clay, M. E., Herman, J., Fleit, H. B., and McCullough, J. (1991) Alloimmune neonatal neutropenia due to an antibody to the neutrophil Fc-γ receptor III with maternal deficiency of CD16 antigen. *Blood* **77,** 1572–1580
33. Ory, P. A., Goldstein, I. M., Kwoh, E. E., and Clarkson, S. B. (1989) Characterization of polymorphic forms of Fc receptor III on human neutrophils. *J. Clin. Investig.* **83,** 1676–1681
34. Edberg, J. C., Redecha, P. B., Salmon, J. E., and Kimberly, R. P. (1989) Human FcγRIII (CD16). Isoforms with distinct allelic expression, extracellular domains, and membrane linkages on polymorphonuclear and natural killer cells. *J. Immunol.* **143,** 1642–1649
35. Huizinga, T. W., Kleijer, M., Tetteroo, P. A., Roos, D., and von dem Borne, A. E. (1990) Biallelic neutrophil Na-antigen system is associated with a polymorphism on the phospho-inositol-linked FcγRIII (CD16). *Blood* **75,** 213–217
36. Fleit, H. B., Wright, S. D., and Unkeless, J. C. (1982) Human neutrophil FcγRIII receptor distribution and structure. *Proc. Natl. Acad. Sci. U. S. A.* **79,** 3275–3279
37. Meknache, N., Jonsson, F., Laurent, J., Guinnepain, M. T., and Daeron, M. (2009) Human basophils express the glycosylphosphatidylinositol-anchored low-affinity IgG receptor FcγRIIIB (CD16B). *J. Immunol.* **182,** 2542–2550
38. Pollard, K. M., Cauvi, D. M., Toomey, C. B., Morris, K. V., and Kono, D. H. (2013) Interferon-γ and systemic autoimmunity. *Discovery Medicine* **16,** 123–131
39. Lazarevic, V., and Glimcher, L. H. (2011) T-bet in disease. *Nat. Immunol.* **12,** 597–606
40. Mócsai, A., Ruland, J., and Tybulewicz, V. L. (2010) The SYK tyrosine kinase: a crucial player in diverse biological functions. *Nature Reviews. Immunology* **10,** 387–402
41. Moretta, L., Webb, S. R., Grossi, C. E., Lydyard, P. M., and Cooper, M. D. (1977) Functional analysis of two human T-cell subpopulations: help and suppression of B-cell responses by T cells bearing receptors for IgM or IgG. *J. Exp. Med.* **146,** 184–200
42. Engelhardt, W., Matzke, J., and Schmidt, R. E. (1995) Activation-dependent expression of low affinity IgG receptors FcγRII(CD32) and FcγRIII(CD16) in subpopulations of human T lymphocytes. *Immunobiology* **192,** 297–320
43. Chauhan, A. K., and Moore, T. L. (2012) Immune complexes and late complement proteins trigger activation of Syk tyrosine kinase in human CD4(+) T cells. *Clin. Exp. Immunol.* **167,** 235–245
44. Schulz, E. G., Mariani, L., Radbruch, A., and Höfer, T. (2009) Sequential polarization and imprinting of type 1 T helper lymphocytes by interferon-γ and interleukin-12. *Immunity* **30,** 673–683
45. Srivastava, S., Pelloso, D., Feng, H., Voiles, L., Lewis, D., Haskova, Z., Whitacre, M., Trulli, S., Chen, Y. J., Toso, J., Jonak, Z. L., Chang, H. C., and Robertson, M. J. (2013) Effects of interleukin-18 on natural killer cells: costimulation of activation through Fc receptors for immunoglobulin. *Cancer Immunology, Immunotherapy : CII* **62,** 1073–1082
46. Greaves, M., Janossy, G., and Doenhoff, M. (1974) Selective triggering of human T and B lymphocytes *in vitro* by polyclonal mitogens. *J. Exp. Med.* **140,** 1–18
47. Sandor, M., Galon, J., Takacs, L., Tatsumi, Y., Mueller, A. L., Sautes, C., and Lynch, R. G. (1994) An alternative Fcγ-receptor ligand: potential role in T-cell development. *Proc. Natl. Acad. Sci. U. S. A.* **91,** 12857–12861
48. Ravetch, J. V., and Bolland, S. (2001) IgG Fc receptors. *Annu. Rev. Immunol.* **19,** 275–290
49. Santana, V., and Turk, J. L. (1975) Binding of aggregated human immunoglobulin to murine thymocytes and T cells through receptors for the Fc region. *Immunology* **28,** 1173–1178
50. Biesecker, G., Katz, S., and Koffler, D. (1981) Renal localization of the membrane attack complex in systemic lupus erythematosus nephritis. *J. Exp. Med.* **154,** 1779–1794
51. Monach, P. A., Hueber, W., Kessler, B., Tomooka, B. H., BenBarak, M., Simmons, B. P., Wright, J., Thornhill, T. S., Monestier, M., Ploegh, H., Robinson, W. H., Mathis, D., and Benoist, C. (2009) A broad screen for targets of immune complexes decorating arthritic joints highlights deposition of nucleosomes in rheumatoid arthritis. *Proc. Natl. Acad. Sci. U. S. A.* **106,** 15867–15872
52. Schroder, K., Hertzog, P. J., Ravasi, T., and Hume, D. A. (2004) Interferon-γ: an overview of signals, mechanisms and functions. *J. Leukocyte Biol.* **75,** 163–189
53. Hu, X., and Ivashkiv, L. B. (2009) Cross-regulation of signaling pathways by interferon-γ: implications for immune responses and autoimmune diseases. *Immunity* **31,** 539–550
54. Ravindran, R., Foley, J., Stoklasek, T., Glimcher, L. H., and McSorley, S. J. (2005) Expression of T-bet by CD4 T cells is essential for resistance to *Salmonella* infection. *J. Immunol.* **175,** 4603–4610
55. Jouvin, M. H., Adamczewski, M., Numerof, R., Letourneur, O., Vallé, A., and Kinet, J. P. (1994) Differential control of the tyrosine kinases Lyn and Syk by the two signaling chains of the high affinity immunoglobulin E receptor. *J. Biol. Chem.* **269,** 5918–5925
56. Krishnan, S., Juang, Y. T., Chowdhury, B., Magilavy, A., Fisher, C. U., Nguyen, H., Nambiar, M. P., Kyttaris, V., Weinstein, A., Bahjat, R., Pine, P., Rus, V., and Tsokos, G. C. (2008) Differential expression and molecular associations of Syk in systemic lupus erythematosus T cells. *J. Immunol.* **181,** 8145–8152
57. Nimmerjahn, F., and Ravetch, J. V. (2007) Fc-receptors as regulators of immunity. *Adv. Immunol.* **96,** 179–204
58. Bulliard, Y., Jolicoeur, R., Windman, M., Rue, S. M., Ettenberg, S., Knee, D. A., Wilson, N. S., Dranoff, G., and Brogdon, J. L. (2013) Activating Fc gamma receptors contribute to the antitumor activities of immunoregulatory receptor-targeting antibodies. *J. Exp. Med.* **210,** 1685–1693
59. Simpson, T. R., Li, F., Montalvo-Ortiz, W., Sepulveda, M. A., Bergerhoff, K., Arce, F., Roddie, C., Henry, J. Y., Yagita, H., Wolchok, J. D., Peggs, K. S., Ravetch, J. V., Allison, J. P., and Quezada, S. A. (2013) Fc-dependent depletion of tumor-infiltrating regulatory T cells co-defines the efficacy of anti-CTLA-4 therapy against melanoma. *J. Exp. Med.* **210,** 1695–1710